International Journal of Heat and Technology
Vol. 43, No. 2, April, 2025, pp. 437-448
Journal homepage: http://iieta.org/journals/ijht

Thermodynamic Behavior Analysis of Lean-Burn Engines Considering Wall Heat Loss and Turbulence-Coupling Effects

Haijun Liu[1*], Zhiguo Liu[2]

[1] School of Mechanical and Traffic Engineering, Ordos Institute of Technology, Ordos 017010, China
[2] Hi-TECH Group Corporation, Beijing 100020, China

Corresponding Author Email: lhj_200610@163.com

https://doi.org/10.18280/ijht.430206

Received: 9 November 2024
Revised: 28 February 2025
Accepted: 17 March 2025
Available online: 30 April 2025

Keywords:
lean-burn engine, wall heat loss, turbulence-coupling effect, numerical simulation, machine learning

ABSTRACT

Against the backdrop of global energy shortages and worsening environmental pollution, lean-burn technology has attracted significant attention for its potential to improve engine thermal efficiency and reduce nitrogen oxide emissions. However, the effects of combustion chamber wall heat loss on in-cylinder temperature and chemical reaction processes, as well as the complex interactions between turbulent flow and combustion stability and pollutant formation, pose challenges for accurate thermodynamic analysis. Existing studies often rely on simplified boundary conditions such as fixed wall temperatures or empirical formulas to model wall heat loss, failing to capture the coupled physical and chemical variations near the wall induced by turbulence. Moreover, common turbulent combustion models typically overlook the changes in turbulence characteristics within boundary layers and the feedback of thermal losses on combustion kinetics, resulting in inaccurate predictions. To address these issues, this study undertakes two key tasks: (1) developing a numerical simulation method for wall heat loss in lean-burn engine combustion chambers that accounts for turbulent energy exchange, near-wall temperature gradients, and chemical reactions, thereby improving the accuracy of heat loss estimation; and (2) integrating machine learning techniques to establish a turbulence-combustion wall model that captures the complex mapping relationships among turbulence, combustion parameters, and wall heat loss within boundary layers. The outcomes of this research will provide a solid theoretical foundation for the optimization of combustion chamber design, combustion system development, and control strategies, offering both engineering significance and academic value for advancing high-efficiency, low-emission engine technologies.

1. INTRODUCTION

With the increasingly severe global energy shortage and environmental pollution problems, the transportation sector has put forward higher requirements for the efficiency and cleanliness of engines [1-3]. As an important means to improve engine thermal efficiency and reduce harmful pollutant emissions [4, 5], lean-burn technology has attracted widespread attention in recent years. This technology, by performing combustion under excess air conditions, can effectively reduce fuel consumption and the formation of nitrogen oxides [6-9]. However, during the actual operation of lean-burn engines, the wall heat loss of the combustion chamber will significantly affect the in-cylinder combustion temperature and chemical reaction process [10], while the coupling effect between turbulent flow and combustion will also have complex impacts on combustion stability and pollutant formation characteristics [11]. Accurately analyzing the thermodynamic behavior of lean-burn engines considering combustion chamber wall heat loss and turbulence-coupling effects has important practical significance for optimizing engine design, improving energy utilization efficiency, and reducing emissions.

Analyzing the thermodynamic behavior of lean-burn engines considering combustion chamber wall heat loss and turbulence-coupling effects has important theoretical and practical application value. From the theoretical perspective, in-depth research on the interaction mechanism between wall heat loss and turbulent flow in the lean-burn process can enrich and improve the thermodynamic theory system of lean-burn engines, and provide new perspectives for revealing energy transfer and flow characteristics under complex combustion environments. In practical applications, accurately mastering the influence law of combustion chamber wall heat loss and turbulence-coupling effects on engine performance can provide a scientific basis for the optimization of combustion chamber structure, combustion system design, and control strategy formulation, which helps to develop lean-burn engines with higher efficiency and lower emissions and promotes the green and sustainable development of the transportation industry.

At present, research on combustion chamber wall heat loss and turbulent combustion in lean-burn engines has achieved certain results, but there are still some shortcomings [12-15].

In the study of wall heat loss, traditional numerical simulation methods usually adopt relatively simplified wall boundary conditions, such as fixed wall temperature or empirical formula-based heat flux models [16], which fail to fully consider the influence of turbulent flow on wall heat transfer and the complex physical and chemical changes near the wall during the combustion process. These simplified treatments lead to low calculation accuracy of wall heat loss and cannot accurately reflect the energy dissipation in the actual combustion process. In terms of turbulent combustion models, some existing models, when dealing with the coupling of turbulence and chemical reaction under lean-burn conditions, often ignore the changes in turbulence flow characteristics within the boundary layer near the wall [17], and the feedback effect of wall heat loss on turbulent combustion kinetics [18]. This causes certain deviations in the prediction of combustion characteristics and pollutant formation in lean-burn engines, making it difficult to meet the engineering demand for high-precision simulations.

The main research content of this paper includes two parts. The first part is the numerical simulation method of wall heat loss in the combustion chamber of lean-burn engines. By establishing a more accurate wall heat transfer model, fully considering the energy exchange between turbulent flow and the wall, as well as the influence of temperature gradients and chemical reactions near the wall during the combustion process on heat loss, a numerical simulation method of wall heat loss suitable for lean-burn environments is developed to improve the calculation accuracy of wall heat loss. The second part is the turbulence-combustion wall model of the combustion chamber boundary layer of lean-burn engines based on machine learning. Combined with machine learning technology, the complex mapping relationship between turbulence flow, combustion parameters, and wall heat loss in the wall boundary layer is explored, and a wall combustion model capable of accurately describing the turbulence-coupling effect is constructed to provide more reliable theoretical support for the thermodynamic behavior analysis of lean-burn engines.

2. NUMERICAL SIMULATION OF WALL HEAT LOSS IN LEAN-BURN ENGINES

2.1 Computational model

Figure 1 shows the schematic diagram of the lean-burn engine structure. In this study, a two-dimensional numerical computation model of the combustion chamber for the lean-burn engine is established. The geometric dimensions of the core combustion region are 2.0 m (length) × 0.6 m (height), and the influence in the depth direction of the combustion chamber is ignored in the simulation to simplify the calculation. The wall of the combustion chamber adopts a multi-layer structure, with the inner layer made of high-temperature resistant alloy material and the outer side covered with a 15 cm thick aluminum silicate refractory fiber blanket as the insulation layer, in order to simulate the thermal insulation characteristics of the actual engine wall. The interior of the combustion chamber is filled with periodically arranged square honeycomb structures to simulate the disturbance effect of turbulence enhancement elements on the combustion flow field. The geometric parameters are consistent with the turbulence generators used in actual engine combustion chambers. The boundary conditions are set as follows: mass flow boundaries are applied at the inlet and outlet of the combustion chamber, and the wall surface adopts a variable heat flux boundary. By applying different external wall heat flux densities, the influence of wall heat loss on the in-cylinder combustion process is investigated. Auxiliary components such as external heat exchangers are not considered in the simulation, with a focus on the thermodynamic behavior of the combustion chamber itself. Figure 2 shows the schematic diagram of the numerical simulation computational model.

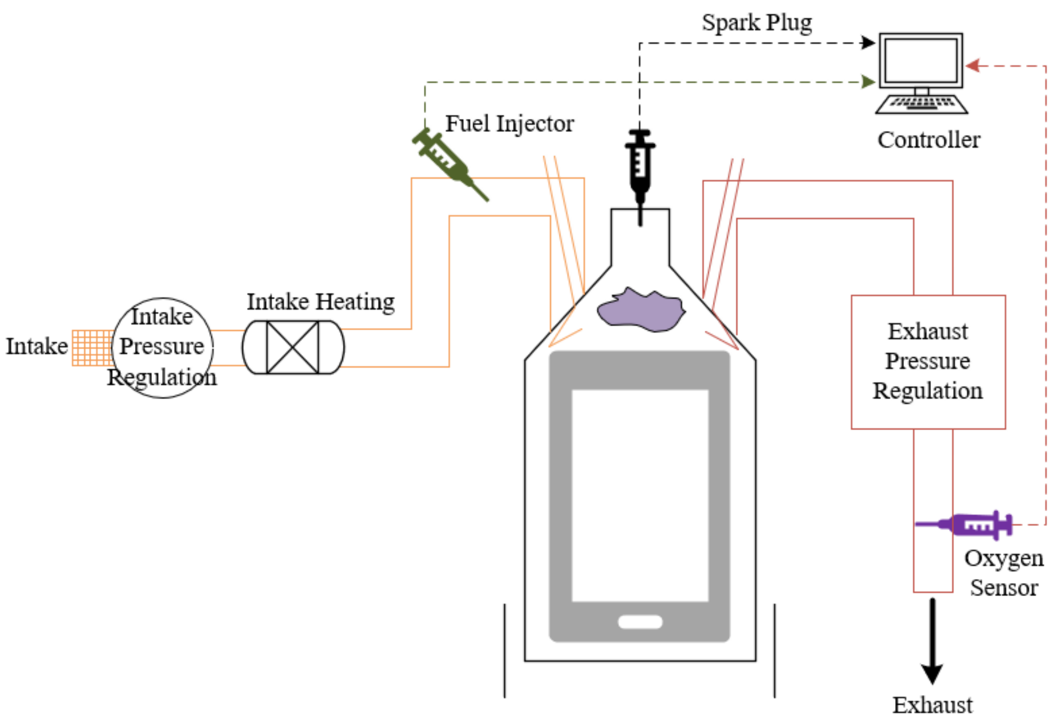

Figure 1. Schematic diagram of the lean-burn engine structure

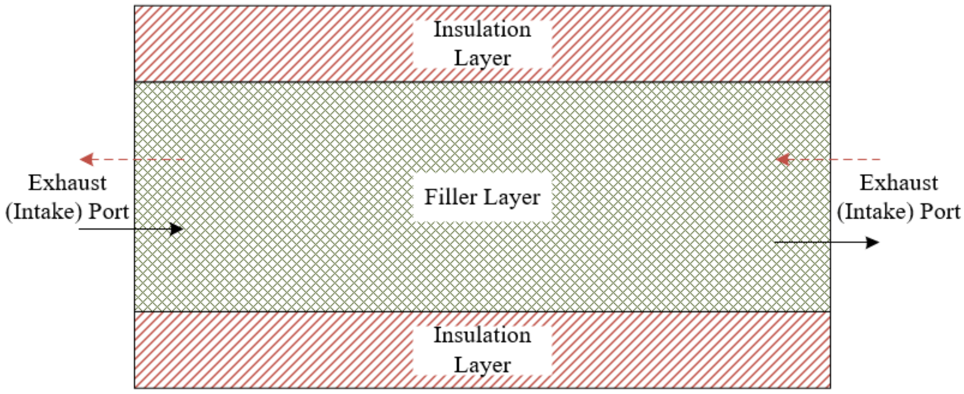

Figure 2. Schematic diagram of the numerical simulation computational model

2.2 Governing equations and boundary conditions

For the complex physicochemical processes in the lean-burn engine combustion chamber, the governing equation system is constructed with thermal-flow-chemical multi-field coupling as the core, aiming to balance computational efficiency and accuracy based on reasonable simplification assumptions. The basic governing equations include the mass conservation equation, momentum conservation equation, and energy conservation equation, which describe the mass transport, turbulent flow, and energy transfer processes of the working fluid in the combustion chamber. The turbulent flow is handled using the Reynolds-Averaged Navier-Stokes (RANS) method, combined with the k-ε two-equation model or the k-ω model to close the turbulent stress terms. The enhanced wall function is used to connect the wall boundary layer with the mainstream flow, capturing the influence of the velocity and temperature gradients near the wall on convective heat transfer. Considering the resistance effect of the ceramic honeycomb filler on the flow, the Brinkman-Forchheimer equation for porous media is introduced to quantify the dissipation effect of the filler structure on turbulent kinetic energy through porosity and internal resistance coefficients, thereby establishing a coupling relationship between flow resistance and wall shear force. In the energy equation, wall heat loss is calculated based on Fourier's law of heat conduction for the solid wall composed of high-temperature alloy and aluminum silicate insulation layers, and is coupled with convective heat transfer between the wall and the combustion flow field, forming a conjugate heat transfer model between fluid and solid. The simplification assumptions include ignoring radiative heat transfer and adopting a single-step global reaction to simplify chemical reaction kinetics, in order to avoid excessive computational complexity and focus on the core coupling effect between wall heat loss and turbulent flow.

The boundary conditions are set closely around the objective of multi-condition investigation of wall heat loss, by stratified setting of inlet, outlet, wall, and filler layer boundaries, to realize targeted simulation of the actual combustion process. The inlet boundary adopts velocity inlet conditions, with precisely given intake velocity, mass fractions of each component, and initial temperature, providing a unified inlet parameter benchmark for different lean-burn conditions. The outlet boundary is set as a pressure outlet, and a backflow condition is applied to limit the fuel component at the outlet, avoiding unphysical backflow interference with the combustion product distribution. The wall boundary adopts the first-type heat flux boundary condition, and the external wall heat flux density is dynamically adjusted according to actual working conditions, achieving quantitative control of wall heat dissipation under different insulation performances or load conditions. This directly investigates the influence of heat loss on the in-cylinder temperature field, combustion rate, and pollutant generation. The filler layer is treated as a porous medium region, and its porosity and resistance coefficient settings are based on experimental measurements and numerical calibration, ensuring that the porous media model accurately reflects the regulation effect of the honeycomb structure on turbulence intensity, flow uniformity, and wall shear force. This further reveals the mapping relationship between turbulence structure variation and wall heat flux density. Through the synergistic effect of the above boundary conditions, a reproducible and adjustable numerical simulation environment is constructed, providing reliable boundary constraints for multidimensional analysis of wall heat loss.

2.3 Initial conditions and solution method

The setting of initial conditions aims to approximate the start-up state of the actual combustion process, and the temperature field of the combustion chamber is precisely initialized through User-Defined Function (UDF). In the Fluent solution environment, the UDF program is used to load the initial temperature distribution of the combustion chamber wall and porous medium filling region. This distribution is based on measured data during the engine cold-start stage or on preliminary thermal equilibrium calculations and includes the temperature gradient characteristics of the high-temperature alloy wall, aluminum silicate insulation layer, and ceramic honeycomb filler. For the combustion flow field, the initial moment sets the inlet velocity, component mass fractions, and gas temperature consistent with the inlet parameters in the boundary conditions, ensuring continuity between the flow field initialization and subsequent boundary conditions. The initial porosity and resistance coefficient of the porous medium region are calibrated through pre-computation, forming the initial flow resistance distribution, and providing a reasonable initial flow field and temperature field basis for the coupled simulation of turbulent flow and wall heat loss.

The numerical solution adopts the unsteady solver of *Fluent* software. The periodic reversal of inlet and outlet boundary conditions is realized by editing the *jou* file, simulating the possible periodic flow in the actual engine. Each reversal cycle includes two stages of forward flow and reverse flow. The duration is determined according to engine operating parameters. During reversal, the inlet and outlet parameters are strictly symmetrically set to ensure the repeatability of flow characteristics. In the solution process, the control equations are discretized using the finite volume method. The pressure-velocity coupling is handled by the SIMPLE algorithm, and the k-ε turbulence model is selected and combined with enhanced wall functions to capture the effects of velocity and temperature gradients in the boundary layer near the wall on heat loss. When the wall heat flux density, combustion chamber temperature field, and component distribution no longer change significantly over several consecutive reversal cycles, the system is considered to have reached a steady state. The results at this point are used to analyze the dynamic law of the coupling effect between wall heat loss and turbulence.

3. MACHINE LEARNING WALL MODEL FOR TURBULENT COMBUSTION IN LEAN-BURN ENGINES

This paper utilizes a direct numerical simulation (DNS) database of the turbulent boundary layer in a lean-burn engine combustion chamber and constructs a fully connected neural network model for the wall stress in the combustion chamber under the large eddy simulation (LES) framework. Figure 3 shows the computational construction schematic of the turbulent combustion boundary layer in the lean-burn engine combustion chamber.

3.1 DNS

For the turbulent combustion process in the boundary layer of the lean-burn engine combustion chamber, DNS is conducted based on the fully compressible Navier-Stokes (N-S) equations to construct benchmark databases for cold-state turbulent boundary layers and turbulent combustion boundary layers. The computational domain is uniformly set as $M_a \times M_b \times M_c$=60×30×30 mm³. The wall adopts an isothermal no-slip boundary condition, i.e., the wall temperature S_Q=800 K, to simulate the actual thermal boundary characteristics of the combustion chamber wall. The free stream parameters match the typical conditions of lean-burn combustion: incoming flow velocity I_∞=100 m/s, temperature S_∞=1200 K, corresponding to a high-speed lean-burn flow field under excess air ratio conditions. By directly solving the complete set of governing equations, including mass, momentum, energy, and species transport, the instantaneous coupling process of turbulent fluctuation, chemical reaction, and wall heat transfer within the boundary layer is accurately resolved, providing high-precision original flow field data for the machine learning model. Specifically, assume that the component index is denoted by subscript j, the viscous stress tensor is denoted by π, the mass fraction of component j is denoted by B_j, the diffusion velocity of component j is denoted by N_j, pressure is denoted by o, the reaction rate of component j is denoted by $\dot{\mu}$, the heat release rate is denoted by $\dot{\mu}_S$, and the enthalpy is denoted by g_t. The Navier-Stokes equation system is expressed as:

$$\frac{\partial \vartheta}{\partial s}+\frac{\partial}{\partial a_u}\left(\vartheta i_u\right)=0 \tag{1}$$

$$\frac{\partial \vartheta i_u}{\partial s}+\frac{\partial}{\partial a_k}\left(\vartheta i_u i_k\right)+\frac{\partial o}{\partial a_u}=\frac{\partial \pi_{uk}}{\partial a_k} \tag{2}$$

$$\frac{\partial \vartheta B_j}{\partial s}+\frac{\partial}{\partial a_u}\left(\vartheta i_u B_j\right)=-\frac{\partial}{\partial a_u}\left(N_{j,u} B_j\right)+\dot{\mu}_j \tag{3}$$

$$\begin{aligned}&\frac{\partial \vartheta g_t}{\partial s}+\frac{\partial}{\partial a_u}\left(\vartheta i_u g_t\right)=\\&\dot{\mu}_S+\frac{Fo}{Fs}+\frac{\partial}{\partial a_u}\left(\eta\frac{\partial S}{\partial a_u}\right)\\&-\frac{\partial}{\partial a_u}\left(\vartheta\sum_{j=1}^{V} N_{j,u} B_j g_{t,j}\right)+\pi_{uk}\frac{\partial i_u}{a_k}\end{aligned} \tag{4}$$

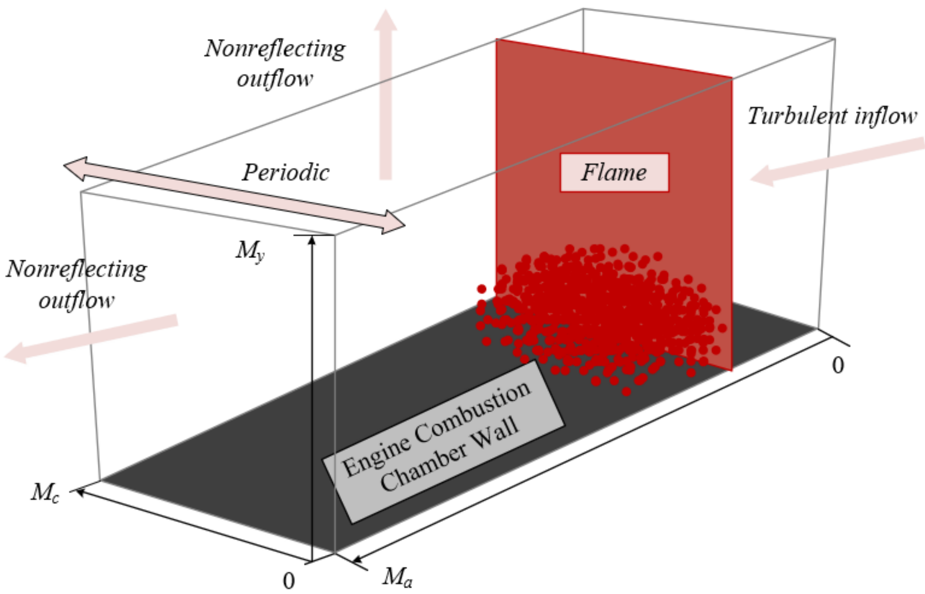

Figure 3. Schematic diagram of the computational construction of the turbulent combustion boundary layer in the combustion chamber of a lean-burn engine

Under cold flow conditions, a refined mesh configuration is adopted: uniform grids are arranged in the streamwise and spanwise directions, i.e., $\triangle a^{IN}$=13 μm, $\triangle c^{IN}$=140 μm; stretched grids are adopted in the wall-normal direction, with the first layer near the wall being $\triangle b^{IN}_{MIN}$=12 μm. The total grid points are $V_z \times V_n \times V_c$=400×260×200. After statistical averaging over 10 time periods $s_k=M_a/I\infty$, a typical turbulent boundary layer flow field is obtained at the streamwise location a=290 mm, with Reynolds number Re_π=360, boundary layer thickness σ_y=7.5 mm, and viscous scale σ_n=20 mm. The non-dimensional grid scales satisfy $\triangle a^{IN+}$=7.5, $\triangle a^{IN+}$=7.5, $\triangle b^{IN}_{MIN}$=0.5, and 10 layers of grids are arranged within the range $b^+ \leq 10$, ensuring accurate resolution of the velocity gradient, temperature gradient, and small-scale turbulent structures near the wall, providing pure flow benchmark data without chemical reaction interference for combustion conditions, and revealing the fundamental coupling mechanism between turbulent fluctuations and wall friction and heat conduction.

In view of the strong coupling characteristics between chemical reactions and turbulence under combustion conditions, a non-uniform mesh refinement strategy is adopted: the total number of grid points is increased to $V_a \times V_b \times V_c$=800×500×400. In the streamwise reaction zone ($0 \leq a \leq 20$ mm), a refined grid ($\triangle a$=63 μm) is set to capture the drastic variation of components and temperature gradients near the flame front; the spanwise direction adopts uniform grid $\triangle c$=63 μm to resolve spanwise turbulent vortex structures; in the wall-normal direction, the first grid layer near the wall is refined to $\triangle b_{MIN}$=10 μm, and the entire boundary layer ($b \leq \sigma_y$) has a grid scale of $\triangle b \leq 63$ μm, meeting the resolution requirements of flame front thickness and turbulence Kolmogorov scale. The computation duration is $3s_k$, ensuring that the distribution of combustion products, heat release rate, and wall heat flux density reach a statistically stable state, obtaining a high-precision dataset containing key parameters such as CH radical concentration, heat release rate fluctuation, and instantaneous wall heat flux, providing data support for revealing the feedback effect of chemical reactions on turbulent structures and wall heat loss in lean combustion boundary layers.

The DNS data of the two working conditions constitute the core training set of the boundary layer turbulent combustion wall model: the cold-state data provide the mapping relationship between wall shear stress, heat flux density under pure turbulent flow and turbulent statistics such as velocity fluctuations and temperature variance; the combustion data include the coupling effects of chemical reaction heat release, component diffusion, and wall heat exchange. By extracting instantaneous flow field parameters such as velocity components, temperature, density, and species mass fractions at different wall-normal positions from the wall to the mainstream region, as well as wall physical quantities such as heat flux density and shear stress, input-output data pairs are constructed: the input includes near-wall turbulent characteristics such as wall friction velocity, temperature gradient, and turbulent kinetic energy, and the output includes wall heat loss rate and combustion product distribution. The dimensionless processing in the dataset ensures the model's generality across different working conditions, while the small-scale fluctuation information resolved by DNS provides the possibility for machine learning to capture nonlinear coupling effects that are difficult for traditional models to describe. Ultimately, the wall model trained on this DNS database can accurately predict the dynamic interaction process between turbulent combustion and wall heat loss in the boundary layer of lean-burn engines, compensating for the inadequacy of traditional RANS models in describing complex coupling effects.

3.2 LES data

This paper adopts the LES method to resolve large-scale turbulent motion in the compressible turbulent combustion process in the boundary layer of a lean-burn engine combustion chamber. Through filtering operations, physical quantities at the coarse grid scale required by LES are extracted from DNS data. The core of the filtering process is to decompose flow field physical quantities into resolvable large-scale components and unresolvable subgrid-scale (SGS) components using a filter function. This filtering operation follows the principles of linear superposition, translational invariance, and locality, ensuring that the physical information of large-scale motion is completely retained, while the influence of small-scale fluctuations is converted into a closure problem for the subgrid model. In lean-burn environments, the filtering process must simultaneously handle density fluctuations of compressible flow, nonlinear heat release from chemical reactions, and strong gradient characteristics of the wall boundary layer, providing reduced-order flow field data containing key features of turbulent combustion for machine learning models. The filtered quantity of physical variable h is defined as:

$$\bar{h}(a) = \int h(a')D(a-a')da' \tag{5}$$

A box filter is used as the scale separation tool, which essentially defines a cubic region in three-dimensional space and averages the flow field information within that region to extract large-scale physical quantities. For the anisotropic characteristics of the combustion chamber boundary layer, the filter adopts uniform grid spacing in the streamwise and spanwise directions to capture long-range vortex structures; in the wall-normal direction, the filter scale is dynamically adjusted according to the boundary layer thickness, with smaller filter units used near the wall to resolve complex velocity and temperature gradients, and appropriately increased scales in the mainstream region to balance computational efficiency. This adaptation strategy ensures that the filter can accurately capture turbulent characteristics at different positions in the boundary layer, providing a unified scale separation basis for subsequent subgrid model construction. Assuming the LES filter is denoted by H and the filter size by $\triangle$, the specific form of the box filter is:

$$H(a) = H(a_1, a_2, a_3) = \begin{cases} 1/\Delta^3, |a_u| \leq \Delta/2, u = 1,2,3 \\ 0, otherwise \end{cases} \tag{6}$$

Since the lean-burn process involves compressible flow, traditional volume-averaged filtering cannot accurately describe mass conservation and energy transport. Therefore, density-weighted filtering is adopted. This method introduces density weighting, using the mass-weighted physical quantity as the large-scale resolvable object, effectively eliminating the interference of density fluctuations on the average result, ensuring the strict validity of the mass conservation equation, and clearly separating the explicit large-scale enthalpy transport and subgrid heat flux in the energy equation. This treatment is critical for resolving the density gradient in the fuel-air mixing zone in the boundary layer, capturing the flame front compression effect, and analyzing the thermal characteristics near the wall, providing purer flow field feature input for machine learning models. The density-weighted filtered quantity of physical variable h is defined as:

$$\bar{\vartheta}\tilde{h}(a)=\int \vartheta h(a')D(a-a')da' \tag{7}$$

After filtering the DNS governing equations, the following expression gives the governing equations obtained for LES:

$$\frac{\partial\bar{\vartheta}}{\partial s}+\frac{\partial}{\partial a_u}\left(\bar{\vartheta}\tilde{i}_u\right)=0 \tag{8}$$

$$\begin{gathered}\frac{\partial\bar{\vartheta}\tilde{i}_u}{\partial s}+\frac{\partial}{\partial a_k}\left(\bar{\vartheta}\tilde{i}_u\tilde{i}_k\right)+\frac{\partial\bar{o}}{\partial a_u}= \\ \frac{\partial}{\partial a_k}\left[\bar{\pi}_{uk}-\bar{\vartheta}\left(\widetilde{i_u i_k}-\tilde{i}_u\tilde{i}_k\right)\right]\end{gathered} \tag{9}$$

$$\begin{gathered}\frac{\partial\bar{\vartheta}\tilde{B}_j}{\partial s}+\frac{\partial}{\partial a_u}\left(\bar{\vartheta}\tilde{i}_u\tilde{B}_j\right)= \\ \frac{\partial}{\partial a_u}\left[\overline{N_{j,u}B_j}-\bar{\vartheta}\left(\widetilde{i_u B_j}-\tilde{i}_u\tilde{B}_j\right)\right]+\overline{\dot{\mu}_j}\end{gathered} \tag{10}$$

$$\begin{gathered}\frac{\partial\bar{\vartheta}\tilde{g}_t}{\partial s}+\frac{\partial}{\partial a_u}\left(\bar{\vartheta}\tilde{i}_u\tilde{g}_t\right)= \\ \overline{\dot{\mu}_S}+\frac{\overline{F_o}}{Fs}+\frac{\partial}{\partial a_u}\left[\bar{\eta}\frac{\partial\tilde{S}}{\partial a_u}-\bar{\vartheta}\left(\widetilde{i_u g_t}-\tilde{i}_u\tilde{g}_t\right)\right]- \\ \frac{\partial}{\partial a_u}\left(\overline{\vartheta\sum_{j=1}^{V}N_{j,u}B_j g_{t,j}}\right)+\pi_{uk}\overline{\frac{\partial i_u}{a_k}}\end{gathered} \tag{11}$$

Steps for Obtaining LES Data

1) Uniform interpolation processing of non-uniform grid data

For the non-uniform grids used in DNS of boundary layers in lean combustion engine combustors, the original DNS data are first converted into uniform grid data through a three-dimensional linear interpolation method, providing a unified spatial discretization basis for subsequent filtering operations. During interpolation, the grid size in the three directions is set to ΔIN=25 μm. This scale is close to the minimum grid size in the DNS case, ensuring that high-frequency fluctuation information of physical quantities such as velocity, temperature, and species concentration near the wall is fully retained. The uniformized grid achieves equal spacing in the streamwise, spanwise, and wall-normal directions, not only eliminating the interference of the original non-uniform grid on the filtering operation but also facilitating the scale separation of anisotropic turbulent structures within the boundary layer in the subsequent LES. This provides a standardized dataset containing complete small-scale features for the machine learning model.

2) Scale separation and data filtering based on three-dimensional box filter

Based on the obtained uniform grid DNS data, a three-dimensional box filter is used to perform scale separation and generate coarse-grid data suitable for LES. The filter size is defined as Δ=30ΔIN, ensuring about 10 LES grids can be reasonably arranged within the combustor boundary layer thickness, satisfying the LES resolution requirements for the boundary layer region. This filtering operation performs arithmetic averaging of DNS data within a cubic region with a side length of Δ centered at each target grid point in the three-dimensional space, decomposing the flow field physical quantities into resolvable large-scale components and SGS components requiring model closure. For the strong gradient characteristics of lean combustion boundary layers, the filtered large-scale data mainly preserve key features such as the mean velocity profile near the wall, temperature stratification, and species mixing rate, while converting the coupling effect of small-scale turbulence fluctuations and wall heat loss into input parameters for the subgrid model.

3.3 Neural network model

For the strong coupling problem of turbulent combustion and wall stress in the boundary layer of lean combustion engine combustors, a fully connected neural network model is constructed based on the LES framework, focusing on the accurate prediction of key components π_{12} and π_{23} of the wall stress tensor π_{uk}. These two components respectively reflect the streamwise-wall-normal and wall-normal-spanwise shear stresses, which directly affect turbulent transport and wall friction characteristics in the momentum equation. The selection of model input variables is based on the physical mechanism of the momentum equation: the streamwise, wall-normal, and spanwise components of velocity and density are used as basic flow parameters, and their gradients, especially the wall-normal velocity gradient $\partial i/\partial b$, are the core driving factors of wall stress and directly determine the instantaneous value of π_{12}. All input variables are taken from the first layer of LES grid away from the wall, which retains the key information of turbulence fluctuations within the boundary layer while avoiding the extreme gradients of the near-wall viscous sublayer that limit the generalization ability of the model, ensuring that the physical correlation between input features and wall stress is effectively captured.

The model training data are derived from the filtered results of cold turbulent boundary layer DNS. A dataset containing the mapping relationship between turbulent flow features and wall stress is constructed through stratified processing of 3.6 million data groups. Three-quarters of the data are used for training and one-quarter for prediction, and cross-validation is used to ensure no intersection between the training and validation sets, avoiding overfitting. The data packaging strategy balances the stability of batch gradient descent with computational efficiency, allowing the model to efficiently learn the statistical patterns in the data. Although the cold-state data do not directly involve combustion reactions, they provide the basic mapping relationship between wall stress and turbulence parameters under pure flow conditions, laying a foundation for the physical mechanism understanding of model extension under combustion conditions, ensuring the model has robustness in the coupling effect of turbulence fluctuations and wall stress in complex combustion environments.

Specifically, suppose the fully connected neural network model is represented by D, and the model parameters are represented by ϕ. The relationship between the model input a_{FI} and output b_{PR} is:

$$b_{PR} = D\left(a_{FI}, \varphi\right) \tag{12}$$

Assuming the correct filtered output variable is b_{FI}, the model parameter ϕ is optimized through the loss function:

$$\hat{\varphi} = ARG\,\underset{\varphi}{MIN}\,M\left(b_{PR}, b_{FI}\right) \tag{13}$$

This study selects mean square error as the loss function:

$$M = \frac{1}{V}\left(b_{u,PR} - b_{u,FI}\right)^2 \tag{14}$$

The model adopts a fully connected neural network architecture with two hidden layers, with 16 neurons in the first layer and 8 neurons in the second layer, gradually reducing dimensions to balance computational complexity and feature extraction capability. The hidden layers use the *ReLU* activation function to effectively solve the gradient vanishing problem and enhance the model's ability to fit nonlinear mappings, i.e., the coupling of density variation and velocity gradient in high-speed lean combustion. The optimization process uses the *Adam* algorithm to dynamically adjust the learning rate and adaptively update parameters, ensuring parameter convergence within a limited training time. This structure design targets the multi-scale features of the combustor boundary layer, i.e., from large eddy motion to subgrid fluctuations, and extracts hierarchical features to convert the velocity field, density field, and their gradient information in the input variables into accurate prediction of wall stress, compensating for the deficiencies of traditional LES models that rely on empirical assumptions.

The model construction is closely aligned with the practical operating conditions of lean combustion engines. Through standardized input and output interfaces, with the first-layer LES grid parameters as input and wall stress components as output, it can be directly embedded into the LES computation process to replace traditional wall stress models. Its efficient computational performance and high-precision prediction capability are especially suitable for turbulent combustion simulations in strong gradient regions within the boundary layer, such as the velocity jump near the flame front and the peak wall heat flux area, and can capture nonlinear effects that are difficult to describe by traditional models.

3.4 Equilibrium model

The construction of the equilibrium model is based on the wall-law theory of turbulent boundary layers, which divides the boundary layer along the wall-normal direction (b direction) into three characteristic regions: the linear sublayer ($b^+ \leq 5$), the buffer layer ($5 < b^+ < 30$), and the logarithmic layer ($b^+ \geq 30$), corresponding to flow characteristics dominated by viscosity, jointly influenced by viscosity and turbulence, and dominated by turbulence, respectively. In the boundary layer of lean combustion engine combustors, high Reynolds number conditions cause significant variation in the thickness of the buffer layer, and temperature gradients induced by wall heat loss further intensify the nonlinearity of the flow. To balance engineering computational efficiency and physical accuracy, the equilibrium model extends the applicable ranges of the linear and logarithmic layers and performs piecewise fitting for the buffer layer: the linear layer is described by the viscous flow assumption to represent the near-wall low-velocity zone ($b^+ \leq 5$), the logarithmic layer is fitted by the classical logarithmic formula to represent the fully developed turbulent zone ($b^+ \geq 30$), and the intermediate buffer layer is connected using polynomial interpolation or piecewise functions, forming a simplified wall-law expression. It is assumed that the dimensionless wall distance is represented by $b^+ = b/\sigma_n = hi_\pi/n$, where the geometric height from the wall is denoted by b, the dynamic viscosity by n, the friction velocity by i_π, where $i_\pi = (\pi_q/\vartheta)^{1/2}$, the main component of wall stress is represented by π_q, the fluid density by ϑ, the dimensionless velocity by $i^+ = i/i_\pi$, the von Karman constant by ν, a constant by Y, and the critical dimensionless distance by b_z. The specific expression is:

$$i^+ = \begin{cases} b^+, b^+ < b_z \\ \ln\left(b^+\right)/\nu + Y, b^+ \geq b_z \end{cases} \tag{15}$$

Aiming at the strong coupling characteristics of the lean combustion boundary layer—namely the interactions among turbulent fluctuations, chemical reaction heat release, and wall heat loss—the equilibrium model introduces correction coefficients to extend the traditional wall-law. In the linear layer, the effect of wall temperature gradient on the viscosity coefficient is considered to modify the slope of the linear velocity distribution; in the logarithmic layer, the von Karman constant and integration constant are adjusted by incorporating fuel species diffusion and heat release rate to reflect the modulation effect of combustion heat release on turbulence intensity. The model particularly focuses on the coupling between wall-parallel and wall-normal shear stress and heat flux, using the direct relationship between the velocity gradient and shear stress in the wall-law to include the wall-normal gradients of temperature and species concentration fields as input parameters, constructing wall boundary conditions that incorporate combustion effects. This model does not require resolving small-scale fluctuations in the buffer layer but instead establishes a mapping between macroscopic flow parameters and wall stress and heat loss through statistical averaging methods. It is applicable to LES frameworks for turbulent combustion simulation and provides prior physical constraints for machine learning models, enhancing their generalization ability and computational efficiency in complex boundary layer environments.

4. EXPERIMENTAL RESULTS AND ANALYSIS

In this study, the simulation physical model system shown in Table 1 is constructed around the core research objective to provide key support for revealing the thermodynamic behavior of lean combustion engines. The turbulence model adopts the LES-Dynamic Smagorinsky model as the core research tool, which separates turbulence scales via LES filtering operations, focusing on resolving large-scale vortex motions, while modeling the influence of small-scale vortices through the dynamic Smagorinsky closure. This matches the analysis needs of the strong coupling effects among turbulence, combustion, and wall heat loss in the study. Meanwhile, the RANS RNG k-ε model is introduced as a comparative reference to verify the advantages of the LES model in capturing the turbulent characteristics of the boundary layer. The hydrogen injection model adopts a simplified injector, focusing on the key characteristics of the fuel injection process. While ensuring computational efficiency, it can reflect the impact of fuel injection on in-cylinder mixing and combustion. The combustion model uses Extended Coherent Flame Model (ECFM), which can effectively describe the flame propagation and structural changes under lean combustion conditions; the ignition model Ignition Statistical Model (ISSIM) accurately simulates the ignition process. These two models together provide a reliable chemical reaction foundation for the numerical simulation of the combustion process. The heat transfer model adopts the Han and Reitz model, emphasizing the energy exchange between turbulent flow and the wall, as well as the effects of temperature gradients and chemical reactions near the wall on heat loss. This echoes the goal of constructing an accurate wall heat transfer model in the first part of the study and provides theoretical support for numerical simulation of wall heat loss. The wall model adopts the standard wall function, which handles the wall boundary layer based on wall-law theory. By simplifying the flow characteristics near the wall, it connects the wall with the main flow region, and while reducing computational complexity, it can describe wall stress and heat flux characteristics. This complements the wall model based on machine learning constructed in the second part, jointly serving the study of turbulent combustion wall characteristics in combustor boundary layers.

Table 1. Physical models for lean combustion engine simulation

Item	Model
Turbulence model	*LES-Dynamic Smagorinsky*
Turbulence model (comparison)	*RANSRNG k-ε*
Hydrogen injection model	Simplified injector
Combustion model	*ECFM*
Ignition model	*ISSIM*
Heat transfer model	*Han and Reitz*
Wall model	Standard wall function

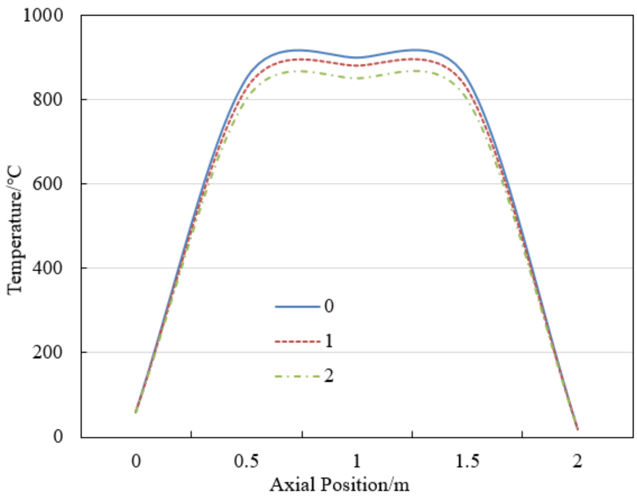

Figure 4. Effect of wall heat flux (0 kW/m², 1 kW/m², 2 kW/m²) on the temperature field of the lean combustion engine combustor

As can be seen from Figure 4, under different wall heat flux conditions, the temperature field of the lean combustion engine combustor shows a trend of first rising and then falling along the axial direction. When the wall heat flux is 0 kW/m² (blue solid line), the temperature peak is relatively high, and the temperature decline rate is slower after the axial position exceeds 1 m; when the wall heat flux increases to 1 kW/m² (red dashed line) and 2 kW/m² (green dotted line), the temperature peak decreases, and the higher the heat flux, the faster the temperature decreases. For example, at the axial position of 1.5 m, the temperature under the wall heat flux of 2 kW/m² is significantly lower than that under 1 kW/m² and 0 kW/m², indicating that the increase in wall heat flux accelerates the heat loss in the combustor, resulting in a more significant overall temperature drop. The above data indicate that wall heat flux has a direct impact on the temperature field of the lean combustion engine combustor. The higher the heat flux, the higher the wall heat loss, and the faster the combustor temperature drops. This phenomenon reveals the mechanism by which wall heat loss changes the temperature gradient through energy exchange, thereby affecting combustion efficiency and stability. The results further verify the importance of the coupling between wall heat loss and turbulence and combustion processes—that is, high wall heat flux accelerates heat dissipation and alters boundary layer turbulence structures and chemical reaction rates.

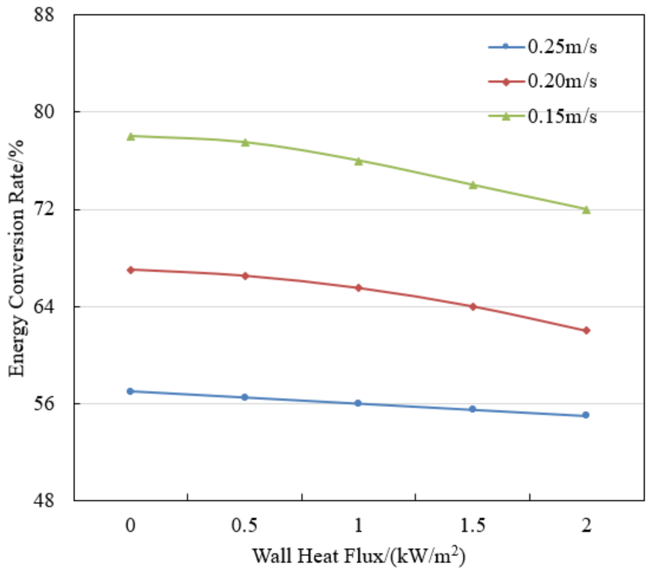

Figure 5. Influence of wall heat loss of lean-burn engine on energy conversion efficiency under different intake velocities (0.25 m/s, 0.2 m/s, 0.15 m/s)

Observing Figure 5, the horizontal axis is wall heat flux, and the vertical axis is energy conversion efficiency. The three curves represent different intake velocities of 0.25 m/s, 0.2 m/s, and 0.15 m/s respectively. As the wall heat flux increases from 0 to 2 kW/m², all three curves show a decreasing trend. Among them, the energy conversion efficiency of 0.15 m/s intake velocity (green line) starts close to 80% and finally drops to about 72%; 0.2 m/s (red line) decreases from about 66% to below 60%; 0.25 m/s (blue line) continues to decline from about 56%. In addition, under the same wall heat flux, the lower the intake velocity, the higher the energy conversion efficiency. For example, when the wall heat flux is 0, the conversion efficiency of 0.15 m/s is significantly higher than that of 0.25 m/s. The data shows that the increase in wall heat flux intensifies energy loss, resulting in a reduction in lean-burn energy conversion efficiency, revealing the mechanism by which wall heat loss weakens combustion efficiency through energy exchange. At the same time, the lower the intake velocity, the higher the energy conversion efficiency, because the low-speed intake allows more sufficient mixing of fuel and air, which is conducive to the combustion reaction. However, the increase in wall heat flux still significantly offsets this advantage. This result further emphasizes the importance of the coupling effect of intake velocity and wall heat flux in the model, i.e., the need to accurately capture their dynamic effects on boundary layer turbulent combustion and energy conversion, to improve the model's predictive capability for the thermodynamic behavior of lean-burn engines, and to provide key evidence for optimizing the combustion process, reducing heat loss, and improving energy utilization.

Table 2. Influence of wall heat loss on temperature field and energy conversion efficiency of lean-burn engine

Heating Power / kW	Maximum Temperature / °C	Average Temperature / °C	Energy Conversion Efficiency / %
0	868.2	658.4	75.6
1.1	915.2	712.6	81.2
2.1	956.3	726.8	83.5

Data in Table 2 show the changes in the temperature field and energy conversion efficiency of the lean-burn engine under different heating powers. When the heating power is 0 kW, the maximum temperature is 868.2°C, the average temperature is 658.4°C, and the energy conversion efficiency is 75.6%; when the heating power increases to 1.1 kW, the maximum temperature increases to 915.2°C, the average temperature reaches 712.6°C, and the conversion efficiency rises to 81.2%; further increasing to 2.1 kW, the maximum temperature reaches 956.3°C, the average temperature 726.8°C, and the conversion efficiency increases to 83.5%. It can be seen that with the increase of heating power, the maximum temperature, average temperature, and energy conversion efficiency all show an upward trend, indicating that heating power has a significant positive impact on the temperature field and energy conversion efficiency. According to the experimental results, the change in heating power reflects the adjustment of wall heat flux density, which in turn affects the temperature gradient near the wall and turbulent energy exchange. The increase in heating power enhances the energy interaction between the wall and the flow field, improves the combustion reaction conditions, makes the combustion more sufficient, thereby increasing temperature and energy conversion efficiency. These experimental data also reveal the internal connection between parameters related to wall heat loss and combustion characteristics, providing a key basis for feature selection and training of the model input.

Observing Figure 6, the horizontal axis is wall heat flux, and the vertical axis is the minimum combustible gas concentration. The three curves represent different intake velocities respectively. As the wall heat flux increases from 0 to 2.0 kW/m², all three curves show an upward trend, indicating that the greater the wall heat flux, the higher the minimum combustible gas concentration required to sustain combustion. At the same time, under the same wall heat flux, the lower the intake velocity, the lower the minimum combustible gas concentration. For example, when the wall heat flux is 2.0 kW/m², the minimum combustible gas concentration corresponding to the intake velocity of 0.15 m/s is significantly lower than those of 0.20 m/s and 0.25 m/s. This data shows that wall heat loss and intake velocity have a significant impact on the minimum combustible gas concentration of the lean-burn engine. An increase in wall heat flux means that wall heat loss is intensified and more heat is dissipated, requiring a higher concentration of fuel gas to maintain the combustion reaction, revealing the mechanism by which wall heat loss affects combustion stability through energy exchange. Meanwhile, the lower the intake velocity, the more sufficient the mixing of fuel and air, the more efficient the combustion process, and the lower the minimum gas concentration required to sustain combustion. This result also emphasizes the importance of intake velocity and wall heat flux as key input parameters. The model needs to accurately capture the coupling influence of the two on the combustion characteristics within the boundary layer to improve the predictive capability for the combustion behavior of lean-burn engines.

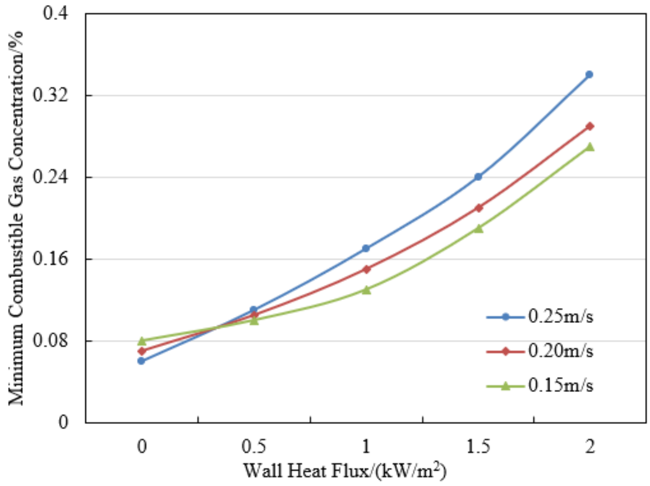

Figure 6. Influence of wall heat loss on minimum combustible gas concentration of lean-burn engine under different intake velocities (0.25 m/s, 0.2 m/s, 0.15 m/s)

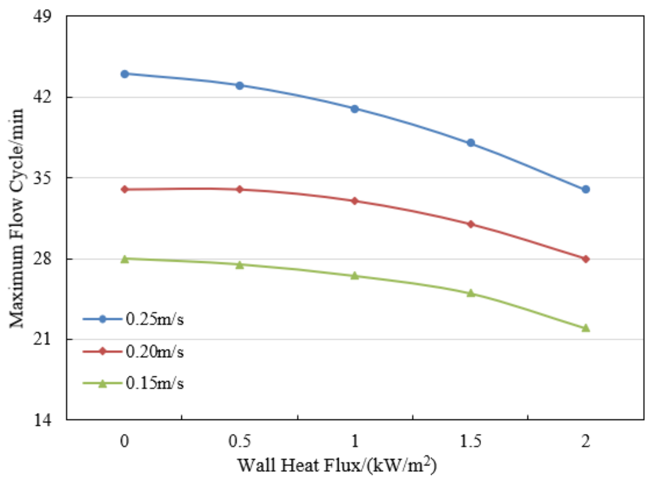

Figure 7. Influence of wall heat loss on maximum flow cycle of lean-burn engine under different intake velocities (0.25 m/s, 0.2 m/s, 0.15 m/s)

Observing Figure 7, the horizontal axis is wall heat flux, and the vertical axis is maximum flow cycle. The three curves represent different intake velocities. As the wall heat flux increases from 0 to 2.0 kW/m², all three curves show a downward trend, indicating that the greater the wall heat flux, the shorter the maximum flow cycle. For example, the maximum flow cycle of intake velocity 0.25 m/s (blue line) decreases from about 42 min to about 35 min, 0.20 m/s (red line) decreases from 35 min to 28 min, and 0.15 m/s (green line) decreases from 28 min to 21 min. In addition, under the same wall heat flux, the higher the intake velocity, the longer the maximum flow cycle. For example, when the wall heat flux is 0, the maximum flow cycle of 0.25 m/s is significantly longer than that of 0.15 m/s. The data shows that the increase in wall heat flux, i.e., the intensification of wall heat loss, will shorten the maximum flow cycle of the lean-burn engine, reflecting the negative impact of wall heat loss on the flow stability of the combustion system, weakening the stability and sustainability of the flow. At the same time, the higher the intake velocity, the longer the maximum flow cycle, indicating that higher intake velocity can provide more kinetic energy to the system, enhance flow stability, and extend the flow cycle.

This result also emphasizes the importance of intake velocity and wall heat flux as key parameters. The model needs to accurately capture the coupling influence of the two on the flow characteristics within the boundary layer to improve the predictive capability for the thermodynamic behavior of the lean-burn engine, providing theoretical basis for optimizing the combustion process, regulating wall heat loss and intake velocity, and further enhancing the stability and efficiency of the combustion system.

Table 3. Influence of wall heat loss on minimum combustible gas concentration and maximum flow cycle of lean-burn engine

Heating Power / kW	**Minimum Combustible Gas Concentration / %**	**Maximum Flow Cycle / min**
0	0.51	21
1.1	0.43	23
2.1	0.32	26

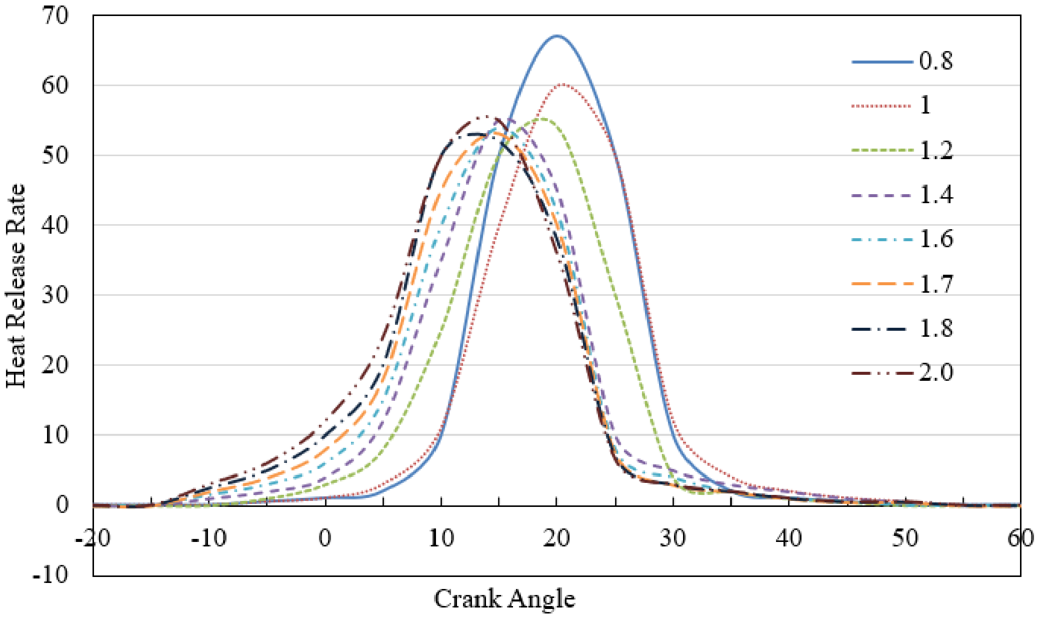

(a) Heat release rate curve

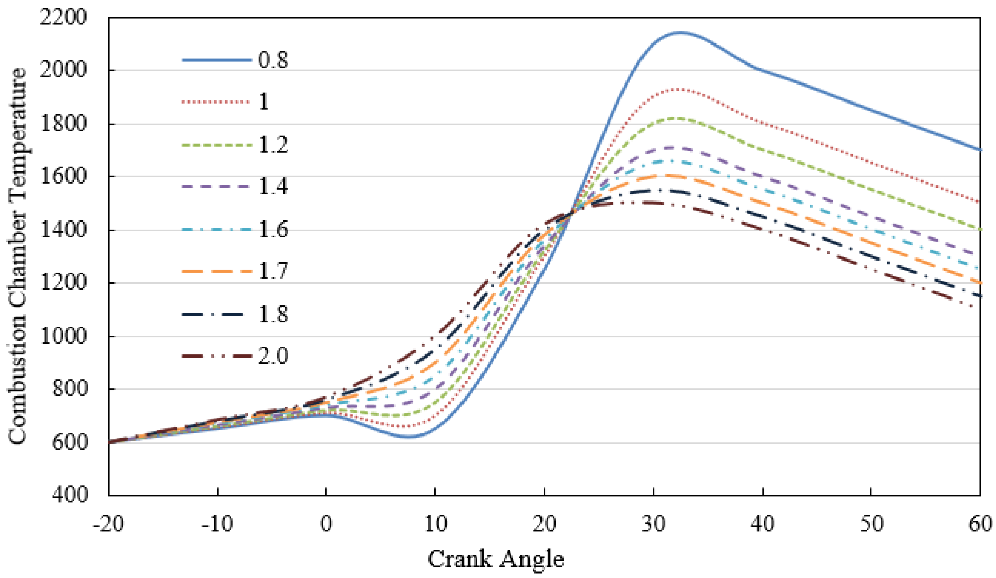

(b) Combustion temperature curve

Figure 8. Characteristics curves of lean combustion in lean burn engine under different combustion limits

Data in Table 3 shows that as the heating power increases from 0 kW to 2.1 kW, the minimum combustible gas concentration of the lean-burn engine gradually decreases from 0.51% to 0.32%, and the maximum flow cycle extends from 21 min to 26 min. Specifically, for every approximately 1.0 kW increase in heating power, the minimum combustible gas concentration decreases by about 0.08%–0.11%, and the maximum flow cycle extends by 2–3 min. This indicates that under the influence of wall heat loss regulation, the minimum gas concentration required to maintain stable combustion decreases as heat loss increases, and the periodicity of the combustion system is significantly enhanced, improving flow stability. The experimental results show that the change in heating power essentially reflects the dynamic adjustment of wall heat flux density, which in turn affects the temperature gradient near the wall and the chemical reaction rate. The decrease in minimum combustible gas concentration is due to the increase in wall heat loss causing the boundary layer temperature to rise, promoting the mixing of fuel and air and the chemical reaction rate, so that the combustion process can be maintained at a lower concentration; while the extension of maximum flow cycle indicates that the coupling effect of wall heat loss and turbulent flow changes the vortex structure and flow resistance within the boundary layer, slows down the flow attenuation rate, and enhances the periodic stability of the combustion system.

Observing Figure 8(a) Heat Release Rate Curve, as the combustion limit increases from 0.8 to 2.0, the peak value of the heat release rate first increases and then decreases, and the crank angle corresponding to the peak gradually shifts backward. For example, when the combustion limit is 0.8, the peak heat release rate is relatively low and appears earlier; when the combustion limit is between 1.2 and 1.6, the peak significantly increases, indicating more intense heat release; however, as the combustion limit further increases, the peak decreases again and the curve width narrows. Figure 8(b) Combustion Temperature Curve shows that when the combustion limit is small, the combustion temperature rises relatively slowly; as the combustion limit increases, the temperature rise rate accelerates, and the peak temperature is higher; but when the combustion limit exceeds 1.6, the temperature rise trend slows down, the increase in peak temperature becomes smaller, and the temperature curves under different combustion limits tend to diverge in the later stage, reflecting differences in combustion process stability. The above curve characteristics indicate that the combustion limit has a significant impact on the combustion characteristics of lean burn engines. Within an appropriate range of combustion limits, the heat release rate and temperature peak are higher, indicating that fuel combustion is more sufficient and intense, energy release is more concentrated, and combustion reaction is promoted. However, when the combustion limit is too high, the growth of heat release rate and temperature slows down, indicating that the combustion process is limited by the lean condition, wall heat loss and turbulent coupling effects lead to a decrease in combustion reaction rate and an increase in heat dissipation, affecting combustion efficiency. These data reveal a complex nonlinear relationship between combustion limit and combustion characteristics, and the model needs to include combustion limit parameters and wall heat loss related variables to accurately capture boundary layer turbulent combustion characteristics, providing more accurate prediction and analysis basis for optimizing the thermodynamic behavior of lean burn engines.

5. CONCLUSION

This paper focused on the coupling problem of turbulent combustion and wall heat loss in the boundary layer of lean burn engine combustion chamber and constructed a wall model based on LES and machine learning. The core research content and results can be summarized as follows:

5.1 Research content and key findings

This study proposed a LES framework applicable to compressible turbulent combustion environments. Through three-dimensional box filter, scale separation of DNS data was carried out, which retained large-scale vortex structures within the boundary layer, while the effects of small-scale fluctuations were transformed into the closure problem of the subgrid model. Aiming at the compressible characteristics of lean combustion, density-weighted filtering was adopted to process the mass conservation and energy transport equations, effectively analyzing the density gradient of the fuel/air mixing layer, flame surface compression effect, and wall heat flow characteristics. On this basis, a fully connected neural network was innovatively introduced to replace traditional empirical models, establishing a nonlinear mapping relationship between subgrid stress/heat flux and local flow field characteristics, realizing high-precision prediction of turbulent combustion wall heat loss within the boundary layer.

5.2 Research value and engineering significance

This study broke through the limitations of traditional LES relying on empirical formulas. Through data-driven methods, it captured the complex coupling effects between wall heat loss and turbulent combustion, providing a more reliable theoretical tool for the thermodynamic behavior analysis of lean burn engine combustion chambers. The specific values are reflected in: (1) Establishing a complete model system that includes turbulence scale separation, compressible flow adaptation, and machine learning integration, significantly improving the simulation accuracy of wall stress and heat loss; (2) Providing key parameter support for engine design, such as revealing the influence laws of wall heat flow on temperature field, energy conversion rate, and combustion stability, assisting in combustion chamber structure optimization and control strategy formulation; (3) Promoting the transformation of turbulent combustion research from “empirical modeling” to “data-physics coupled modeling,” providing a universal method framework for multi-field coupling problems in complex combustion environments.

5.3 Research limitations and future directions

The current study still has the following shortcomings: (1) Model training relies on DNS data of cold-state turbulent boundary layer, with insufficient coverage of combustion conditions containing chemical reactions, and has not yet fully revealed the dynamic interaction mechanism between fuel component diffusion, heat release rate, and wall heat loss; (2) The correlation analysis between the filtering scale of LES and the input features of machine learning is not in-depth enough, and the generalization ability of the model under extreme lean combustion conditions needs to be verified; (3) Practical engineering factors such as wall material property changes and carbon deposition have not been considered in the impact on heat loss.

Future research can be expanded from the following directions: (1) Integrate DNS data under combustion conditions to construct machine learning models coupled with multi-physical fields, improving the analysis capability of complex chemical reactions and turbulence interactions; (2) Combine experimental measurements to verify and calibrate the model, enhancing its engineering applicability; (3) Explore lightweight neural network structures to reduce computational cost and improve the application potential of the model in real-time simulation; (4) Carry out multi-objective optimization research on wall heat loss and engine cycle efficiency and emission characteristics, promoting the transformation of research results into practical engineering applications.

ACKNOWLEDGMENT

This paper was funded by the Science and Technology Project of University in Inner Mongolia Autonomous Region (Grant No.: NJZZ22227).

REFERENCES

[1] Stotsky, A. (2005). Computationally efficient filtering algorithms for engine torque estimation. Proceedings of the Institution of Mechanical Engineers, Part D: Journal of Automobile Engineering, 219(9): 1099-1107. https://doi.org/10.1243/095440705X34711

[2] Levario-Medina, S., Valencia-Ortega, G., Arias-Hernandez, L.A. (2019). Thermal optimization of Curzon-Ahlborn heat engines operating under some generalized efficient power regimes. The European Physical Journal Plus, 134(7): 348. https://doi.org/10.1140/epjp/i2019-12711-2

[3] Šauperl, I., Wimmer, A., Dimitrov, D., Zelenka, J., Pirker, G., Schnessl, E., Winter, H. (2018). LDM COMPACT-A methodology for development of gas engines for use with low environmental impact non-natural gas. Journal of Mechanical Engineering/Strojniški Vestnik, 64(12): 743-752. https://doi.org/10.5545/sv-jme.2018.5344

[4] Gong, C., Li, Z., Sun, J., Liu, F. (2020). Evaluation on combustion and lean-burn limit of a medium compression ratio hydrogen/methanol dual-injection spark-ignition engine under methanol late-injection. Applied Energy, 277: 115622. https://doi.org/10.1016/j.apenergy.2020.115622

[5] Park, C., Lee, S., Yi, U. (2016). Effects of engine operating conditions on particle emissions of lean-burn gasoline direct-injection engine. Energy, 115: 1148-1155. https://doi.org/10.1016/j.energy.2016.09.051

[6] Iwakuni, H., Takami, A., Komatsu, K. (1999). Development of lean NOx catalyst for lean burn gasoline engine. In Studies in Surface Science and Catalysis, 121: 251-256. https://doi.org/10.1016/S0167-2991(99)80075-5

[7] Park, J., Choi, J. (2017). A numerical investigation of lean operation characteristics of spark ignition gas engine fueled with biogas and added hydrogen under various boost pressures. Applied Thermal Engineering, 117: 225-234. https://doi.org/10.1016/j.applthermaleng.2017.01.115

[8] Cho, H.M., He, B.Q. (2008). Combustion and emission characteristics of a lean burn natural gas engine. International Journal of Automotive Technology, 9: 415-422. https://doi.org/10.1007/s12239-008-0050-5

[9] Sapra, H., Godjevac, M., De Vos, P., Van Sluijs, W., Linden, Y., Visser, K. (2020). Hydrogen-natural gas combustion in a marine lean-burn SI engine: A comparitive analysis of Seiliger and double Wiebe function-based zero–dimensional modelling. Energy Conversion and Management, 207: 112494. https://doi.org/10.1016/j.enconman.2020.112494

[10] Kawaguchi, A., Wakisaka, Y., Nishikawa, N., Kosaka, H., Yamashita, H., Yamashita, C., Tomoda, T. (2019). Thermo-swing insulation to reduce heat loss from the combustion chamber wall of a diesel engine. International Journal of Engine Research, 20(7): 805-816. https://doi.org/10.1177/1468087419852013

[11] Gao, Z., Lee, C. (2010). A numerical study of turbulent combustion characteristics in a combustion chamber of a scramjet engine. Science China Technological Sciences, 53: 2111-2121. https://doi.org/10.1007/s11431-010-3088-3

[12] Zhang, X., Wang, Z., Chen, M., Qiu, T. (2023). Experimental study combustion behavior of wallpapers under different external heat fluxes. Journal of Thermal Analysis and Calorimetry, 148(6): 2645-2656. https://doi.org/10.1007/s10973-022-11876-6

[13] Trisjono, P., Kleinheinz, K., Pitsch, H., Kang, S. (2014). Large eddy simulation of stratified and sheared flames of a premixed turbulent stratified flame burner using a flamelet model with heat loss. Flow, Turbulence and Combustion, 92: 201-235. https://doi.org/10.1007/s10494-013-9522-4

[14] Babaelahi, M., Abdi, S. (2025). Enhanced polytropic stirling engine thermal model (EPSETM): Integrating empirical effects of intermolecular Van der Waals forces on internal energy change and fluid flow dispersion heat loss in the regenerator. Energy Sources, Part A: Recovery, Utilization, and Environmental Effects, 47(1): 6999-7016. https://doi.org/10.1080/15567036.2025.2477837

[15] Rebhan, E. (2002). Efficiency of nonideal Carnot engines with friction and heat losses. American Journal of Physics, 70(11): 1143-1149. https://doi.org/10.1119/1.1501116

[16] Sharkov, A.V., Korablev, V.A., Makarov, D.S., Minkin, D.A., Nekrasov, A.S., Gordeichik, A.A. (2016). Measurement of high-density heat flux using an automated installation. Measurement Techniques, 59: 67-69. https://doi.org/10.1007/s11018-016-0918-0

[17] Chrigui, M., Gounder, J., Sadiki, A., Janicka, J., Masri, A.R. (2013). Acetone droplet behavior in reacting and non reacting turbulent flow. Flow, Turbulence and Combustion, 90: 419-447. https://doi.org/10.1007/s10494-012-9441-9

[18] Boileau, M., Staffelbach, G., Cuenot, B., Poinsot, T., Bérat, C. (2008). LES of an ignition sequence in a gas turbine engine. Combustion and Flame, 154(1-2): 2-22. https://doi.org/10.1016/j.combustflame.2008.02.006